THE JOURNAL OF BIOLOGICAL CHEMISTRY VOL. 286, NO. 39, pp. 33931–33941, September 30, 2011

Plant-Specific Cation/H^+ Exchanger 17 and Its Homologs Are Endomembrane K^+ Transporters with Roles in Protein Sorting*[S]

Received for publication, May 5, 2011, and in revised form, July 8, 2011 Published, JBC Papers in Press, July 27, 2011, DOI 10.1074/jbc.M111.252650

Salil Chanroj[‡], Yongxian Lu (路永憲)[‡1], Senthilkumar Padmanaban[‡], Kei Nanatani (七谷圭)[§], Nobuyuki Uozumi (魚住信之)[§], Rajini Rao[¶], and Heven Sze (斯海文)[‡2]

From the [‡]Department of Cell Biology and Molecular Genetics and the Maryland Agricultural Experiment Station, University of Maryland, College Park, Maryland 20742, the [¶]Department of Physiology, Johns Hopkins University School of Medicine, Baltimore, Maryland 21205, and the [§]Department of Biomolecular Engineering, Graduate School of Engineering, Tohoku University, Sendai 980-8579, Japan

The complexity of intracellular compartments in eukaryotic cells evolved to provide distinct environments to regulate processes necessary for cell proliferation and survival. A large family of predicted cation/proton exchangers (CHX), represented by 28 genes in *Arabidopsis thaliana*, are associated with diverse endomembrane compartments and tissues in plants, although their roles are poorly understood. We expressed a phylogenetically related cluster of CHX genes, encoded by *CHX15–CHX20*, in yeast and bacterial cells engineered to lack multiple cation-handling mechanisms. Of these, CHX16–CHX20 were implicated in pH homeostasis because their expression rescued the alkaline pH-sensitive growth phenotype of the host yeast strain. A smaller subset, CHX17–CHX19, also conferred tolerance to hygromycin B. Further differences were observed in K^+- and low pH-dependent growth phenotypes. Although CHX17 did not alter cytoplasmic or vacuolar pH in yeast, CHX20 elicited acidification and alkalization of the cytosol and vacuole, respectively. Using heterologous expression in *Escherichia coli* strains lacking K^+ uptake systems, we provide evidence for K^+ (^{86}Rb) transport mediated by CHX17 and CHX20. Finally, we show that CHX17 and CHX20 affected protein sorting as measured by carboxypeptidase Y secretion in yeast mutants grown at alkaline pH. In plant cells, CHX20-RFP co-localized with an endoplasmic reticulum marker, whereas RFP-tagged CHX17–CHX19 co-localized with prevacuolar compartment and endosome markers. Together, these results suggest that in response to environmental cues, multiple CHX transporters differentially modulate K^+ and pH homeostasis of distinct intracellular compartments, which alter membrane trafficking events likely to be critical for adaptation and survival.

The dynamic endomembrane system of eukaryotic cells is emerging as a critical and central coordinator in cell development, growth, signaling, and adaptation to stress (1, 2). Recent studies have illustrated the increasing complexity of intracellular compartments that sort proteins and membranes in the anterograde or retrograde direction through the biosynthetic and/or the endocytic pathway. Such compartments probably evolved to provide distinct environments in a temporal manner for specific biochemical reactions and protein-protein interactions necessary for cell proliferation and survival (3), yet the mechanisms that regulate the internal and external environment of these endomembrane compartments in plants are not well understood. In plants, the dynamic endomembrane affects cell polarity, cytokinesis, cell wall formation and stress tolerance (1, 4).

Endomembranes of eukaryotic cells, including those from yeast, mammals, and plants, share several transporters in common, indicating that the mechanisms controlling the physicochemical environment of diverse intracellular compartments are conserved in general. The most prominent is the H^+-pumping vacuolar ATPase, which acidifies intracellular compartments, including yeast (5) and plant vacuoles (6), *trans*-Golgi network (7), clathrin-coated vesicles, lysosomes, and endosomes of diverse animal cells (8). Because the V-ATPase is an electrogenic H^+-pump, acidification of membrane vesicles occurs only if counter ions, such as anions, enter to dissipate the electrical potential (9). Several alkali-cation/proton exchangers belonging to the cation-proton antiporter 1 (CPA1) family have been found in endomembranes of eukaryotes (2, 10, 11). Examples include vacuolar ScNHX1 of yeast, six Na^+/H^+ exchanger (NHX)[3] genes in *Arabidopsis*, and NHE6 to -9 in humans. Alkali-cation/proton exchangers provide a leak pathway for H^+ and thus modulate lumenal pH and cation homeostasis within the endomembrane system, where they have profound effects on vesicle biogenesis and trafficking in cells (2).

In plants, NHX1 represents the best characterized member of the CPA1 family. NHX1 was initially characterized as a vac-

* This work was supported, in whole or in part, by National Institutes of Health Grant R01DK054214 (to R. R.). This work was also supported by National Science Foundation Grant IBN0209788 and United States Department of Energy Grant BES DEFG0207ER15883 (to H. S.), Japan Society for the Promotion of Science Grants-in-Aid for Scientific Research 22020002 and 22380056 (to N. U.), and a Royal Thai Government Fellowship (to S. C.).

⌘ *Author's Choice*—Final version full access.

[S] The on-line version of this article (available at http://www.jbc.org) contains supplemental Tables S1–S10, Figs. S1–S10, and additional methods and references.

[1] Present address: Carnegie Inst. for Science, Dept. of Plant Biology, 260 Panama St., Stanford, CA 94305.

[2] To whom correspondence should be addressed: 0120 Bioscience Research Bldg. (413), Dept. of Cell Biology and Molecular Genetics, University of Maryland, College Park, MD 20742. Tel.: 301-405-1645; Fax: 301-314-1248; E-mail: hsze@umd.edu.

[3] The abbreviations used are: NHX, Na^+/H^+ exchanger; CHX, cation/H^+ exchanger; BCECF, (2′,7′-bis(2-carboxyethyl)-5(6)-carboxyfluorescein acetoxymethyl ester; CPY, carboxypeptidase Y; HygB, hygromycin B; PM, plasma membrane; PVC, prevacuolar compartment(s); SGM, synthetic glycerol-mannitol; ER, endoplasmic reticulum; CCCP, carbonyl cyanide *m*-chlorophenylhydrazone.

uolar Na^+/H^+ exchanger, although later findings broadened cation selectivity to include K^+ (11–15). In addition to vacuole and prevacuolar endosomes, plant NHX isoforms are found in other endomembranes. Tomato LeNHX2, a homolog of AtNHX5/6, is a K^+-selective H^+ exchanger localized to the Golgi and endosomes (15). Recently, AtNHX5 and AtNHX6 were localized to Golgi or the *trans*-Golgi network and shown to play a role in cell expansion because double mutants were dwarfed (16). In addition, NHX7/SOS1, a plasma membrane member, is important for conferring salt tolerance probably by controlling long distance Na^+ transport (17). These findings show that members of the plant NHX family modulate Na^+ and K^+ homeostasis at various endomembrane compartments as well as the plasma membrane.

Given the multiplicity of plant NHX genes, it was surprising to discover a large family of putative cation/H^+ exchangers (CHXs) (18) in a distinct CPA2 superfamily, sharing sequence similarity to bacteria NhaA and KefB (10). Intriguingly, most of the eukaryotic genes in CPA2 come from plants and fungi (10, 18). Metazoan genomes each carry only two CPA2 members, NHA1 and NHA2, that appear to have risen by gene duplication (10). Human NHA2 shows broad tissue distribution and confers tolerance to Na^+ and Li^+ but not to K^+, when expressed in yeast (19). In striking contrast, *Arabidopsis thaliana* alone possesses 28 CHX genes, and the rice genome has 17 members (18). The multiplicity of CHX genes in plants raised questions about their transport activity and their biological functions.

Arabidopsis CHX genes are differentially expressed in plant cell types (18, 20). *AtCHX20* is preferentially expressed in leaf guard cells. Null mutants of *Atchx20* were impaired in light-induced stomatal opening, indicating a role in osmoregulation (21). *AtCHX21* and *AtCHX23* play overlapping roles in pollen tube guidance because double mutants failed to target ovules and exhibited impaired pollen fertility (22). *AtCHX17*, expressed in roots, appears to have a role in K^+ homeostasis because mutants had decreased K^+ content (23). *CHX17* and *CHX20* were able to promote growth of alkaline-sensitive yeast strains on medium at pH 7.5 (21, 24). However, their transport activity, membrane localization, and cellular roles remain unclear.

Here, we have used yeast and *Escherichia coli* as model organisms to distinguish between shared and isoform-specific activities of *Arabidopsis CHX16* to *-20*. These studies provide evidence for dissimilar roles of CPA1 and CPA2 members of cation/proton exchangers and reveal the complexity of multiple plant CHX transporters. We show that CPA2 members transport K^+ and appear to modulate K^+ and pH homeostasis of diverse intracellular organelles that alter endomembrane trafficking.

MATERIALS AND METHODS

Yeast, Bacterium, and Plant—Saccharomyces cerevisiae strains used here are shown in supplemental Table S1. Untransformed strains were grown in YPAD medium. *Escherichia coli* strain LB2003 (*trkA*Δ, *kup1*Δ, *kdpABCDE*Δ) (22, 25) was grown in YTMK medium at pH 7.3 (supplemental Table S7*B*). *Arabidopsis thaliana* (Col-0) plants were grown on Miracle-Gro® potting mix with continuous light at 50 microeinsteins m^{-2} s^{-1}, 21 °C, and 65% humidity.

cDNA Cloning and Plasmid Preparation—CHX15 to *CHX19* ORFs were PCR-amplified (supplemental Table S2) from cDNA obtained by reverse transcription of seedling RNA and cloned into Gateway pDONR221 as described for *CHX20* (21). *CHX17* was amplified from a cDNA clone in pSMCHX17. DNA was recombined into entry and destination vectors for expression in yeast (supplemental Tables S3 and S4) using Gateway LR Clonase II Enzyme Mix (supplemental Table S5). For empty vector, a 90-bp sequence (supplemental Table S3) was inserted into Gateway pENTR/D-TOPO. Plasmid was amplified in *E. coli* strain DH5α (18265-017, Invitrogen) and purified with a miniprep kit (27106, Qiagen). For expression in *E. coli*, *CHX17* and *CHX20* were amplified from entry vectors, pECHX17 and pECHX20 (supplemental Table S3), using I-proof DNA polymerase (172-5331, Bio-Rad) and suitable primers (supplemental Table S6) and subcloned in plasmid pPAB404 (26). Plasmids were amplified in *E. coli* NEB10β (C3019H, New England Biolabs) and purified as above.

Yeast Transformation and Functional Assays—Yeast was transformed with the lithium acetate method (27) and selected on YNB medium containing adenine and required amino acids at pH 5.8. Growth was synchronized in YNB without a carbon source unless galactose was added to induce gene expression. Cells were normalized in water or K^+-free YNB to A_{600} of 0.2. Five μl of each serial dilution was spotted onto YNB or SDAP medium with 2% glucose or 2% galactose (supplemental Table S7*A*) and incubated at 30 °C for 3–5 days. Drop test media had 20 mM MES, and pH was adjusted to 7.5 with arginine or to acidic pH values with glutamic acid. K^+ concentration was adjusted with KCl.

pH_{cyt} and pH_{vac} Determination—To monitor cytosolic pH, we used a pH-sensitive GFP variant, superecliptic pHluorin (GenBank™ accession number AY533296) from Dr. Miesenbock (Yale University). A destination vector (pDYpH) harboring *pHluorin* was generated with or without a CHX gene by PCR-directed *in vivo* homologous recombination in yeast (28) (supplemental Fig. S2A) using primers shown in supplemental Table S8. To measure cytosolic pH, an aliquot of normalized cells were mixed with YNB medium supplemented with 2% glucose at varied pH and K^+ concentration. The plate was immediately placed in a multimode plate reader (BMG FLUOstar Optima model, BMG Labtechnologies) set to 30 °C. Emission at 460 nm (F_{460}) and 510 nm (F_{510}) was read using excitation at 400 nm. F_{510}/F_{460} was converted to pH units using a pH calibration curve as described by Brett *et al.* (29).

To estimate vacuolar pH (30), cells were loaded with 50 μM 2′,7′-bis(2-carboxyethyl)-5(6)-carboxyfluorescein acetoxymethyl ester (BCECF) (B8806, Sigma) and mixed with YNB medium supplemented with 2% glucose at varied pH and K^+ concentration. The ratio of fluorescence at 530 nm was determined at F_{ex492}/F_{ex460} and converted to pH units using a pH calibration curve (see supplemental Methods).

Measuring Carboxypeptidase Y Secretion—Twenty μl of normalized cells was added to a white opaque ELISA plate (15042, Pierce) containing 180 μl of YNB-galactose medium, pH 5.5, supplemented with 4 mM K_2SO_4 or 8 mM KOH (pH 7.3). Plates

were incubated at 30 °C to early log phase. Cells were removed, and CPY attached to plates were determined using mouse anti-CPY (1:1000; A-6428, Invitrogen), followed by anti-mouse IgG conjugated with horseradish peroxidase (31430, Thermo Scientific). Chemiluminescence from 10 cycles was pooled. Relative luminescence units were normalized to cell density at A_{600} (see supplemental Methods).

E. coli Growth and $^{86}Rb(K^+)$ Transport—*E. coli* strain LB2003 was transformed with pPAB404 *KAT1* (31), CHX17, or CHX (20) by heat shock. Transformants were selected on YTMK or synthetic-glycerol-mannitol (SGM)-KN medium (supplemental Table S7*B*) with 50 μg/ml ampicillin (32). Cell growth at A_{600} was tested on medium with 50 μg/ml ampicillin, 0.5 mM IPTG, and varied cations or pH (see supplemental Methods). ^{86}Rb (K^+) transport was determined by filtration using a 0.45-μm nitrocellulose membrane (Protran BA85, Whatman). Freshly transformed cells were K^+-depleted for 2 h and normalized. A typical reaction of 750 μl contained cells at A_{600} 0.4 (~2.5×10^8 cells/ml), 0.5 mM isopropyl β-D-thiogalactopyranoside, 0.6 mM RbCl, ^{86}Rb (0.5 μCi/ml) in a 0.25× basal SGM with 80 mM glycerol, 10 mM MES, and 10 mM MOPS, pH 6.2. Cells and ^{86}Rb were added to start the reaction, and an aliquot was counted to convert dpm to nmol.

Transfection of Plant Protoplast—Cells without cell walls were isolated from 3-week-old leaves and transfected by the PEG-Ca method (33, 34). Plasmids containing GFP or RFP fusion constructs are shown in supplemental Table S9. Transfected cells were incubated in the dark at 22 °C for 18–24 h. Efficiency of transformation with a single gene is ≥50% and with two genes is less due to differential signals and gene expression (see supplemental Methods).

Microscopy—Fluorescent proteins in cells were examined with a Zeiss LSM510 confocal microscope (Carl-Zeiss, Germany) and C-Apochromat ×63 numerical aperture/1.2 water immersion lens. Five μl was dropped onto a slide using two 0.5-mm parafilm strips as spacers between slide and coverglass. To enhance cell density, protoplasts were concentrated >10-fold by centrifugation. Filter sets for excitation and emission are as follows: 488 nm/BP505–530 nm for GFP; 543 nm/BP560–615 nm for RFP; 543 nm/LP650 nm for chlorophyll, and 633 nm for bright field. Signals were captured in multichannel mode. Images were analyzed and processed in a Zeiss LSM image browser (Carl-Zeiss). Yeasts expressing GFP were grown overnight in YNB medium, pelleted, and incubated in YPAD for 4 h at 30 °C. Before microscopy, cells were incubated for 10 min in 10 μM FM4-64 (T-3166, Invitrogen), washed with 2% sucrose, and suspended in 0.05% agarose. The filter set for FM4-64 is 488 nm (excitation)/LP650 nm (emission).

RESULTS

Phylogenetic Relationship of AtCHX, ScKHA1, and NHX1—According to cDNA sequences, the deduced proteins CHX15–CHX20 have a hydrophobic domain with 12 transmembrane spans at the N-terminal half (427–433 residues) and a hydrophilic C tail of 372–409 residues (supplemental Fig. S1) (18). Phylogenetic analysis has revealed that CHX15–CHX20 are tightly clustered away from yeast KHA1 within the CPA2 family (Fig. 1); however, the CHX cluster and ScKHA1 are both clearly separated from the CPA1 family represented by yeast and *Arabidopsis* NHXs (10). Although ScKHA1 has only 38–41% overall similarity to CHX15–CHX20, the transmembrane domain shared 60% homology (supplemental Fig. S1 and Table S10). Thus, ScKHA1 is considered orthologous to AtCHX15–AtCHX20.

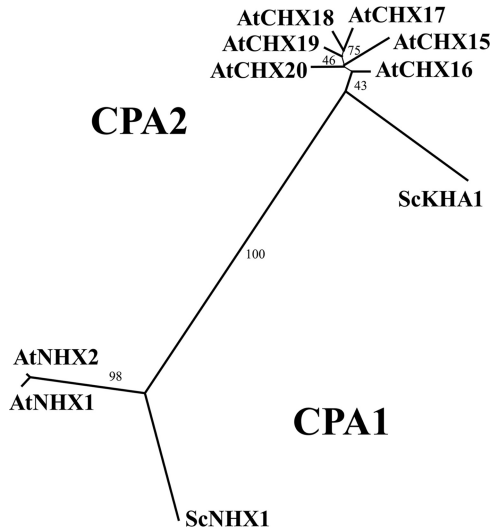

FIGURE 1. ***Arabidopsis* CHX15 to -20 are homologs of yeast KHA1.** AtCHX15–AtCHX20 and ScKHA1 (YJL094C) form a cluster within the CPA2 family, and ScNHX1 (YDR456W) and AtNHX1–2 (At5g27150, At3g05030) cluster within the CPA1 family. AtCHX genes identified by AGI no. At2g13620 (CHX15), At1g64170 (CHX16), At4g23700 (CHX17), At5g41610 (CHX18), At3g17630 (CHX19), and At3g53720 (CHX20) encode proteins of 86.9–91.5 kDa (supplemental Fig. S1). Alignment was processed by ClustalX version 2.0. Values indicate the percentage of times (%) that each branch topology was found in 10,000 replicates in an unrooted tree.

AtCHX16–AtCHX20 Confer Yeast Growth at Alkaline pH—We tested CHX15–CHX20 function in a panel of yeast mutants variously defective in Na^+ extrusion and $K^+(Na^+)/H^+$ antiport (Fig. 2*A*). Cation/proton antiporters maintain cellular pH homeostasis and growth in response to large perturbations in external pH. Thus, yeast strain KTA40-2 proliferated at pH 5.6 but failed to grow at pH 7.5. We showed that KTA40-2 expressing *CHX16*, *-17*, *-18*, *-19*, or *-20* recovered tolerance to alkaline pH, similar to the AXT3 strain that expresses the endogenous *ScKHA1* (Fig. 2*B*, *right*). Similar results were obtained when *CHX17* or *CHX20* was expressed in the single *kha1*Δ mutant at low K^+ (Fig. 2*E*). Alterations in membrane potential and membrane trafficking significantly influence sensitivity to the cationic drug hygromycin B (35, 36). KTA40-2 was shown to be sensitive to HygB (100 μg/ml) at pH 5.6 (Fig. 2*B*, *middle*). Interestingly, only CHX17, -18, or -19 conferred resistance to the drug (Fig. 2*B*), similar to ScKHA1, whereas CHX15, CHX16, and CHX20 did not. CHX15 was unable to restore growth under any of the conditions tested. These results suggest that multiple CHX genes share a role in pH homeostasis, although they differ in the ability to confer hygromycin B resistance.

AtCHX17 and AtNHX1 Have Distinct yet Overlapping Functions—Yeast strains with endogenous *ScNHX1* but lacking *ScKHA1* (LMB01) grew poorly on alkaline medium, compared with strains expressing either *AtCHX17* (in KTA40-2) or *ScKHA1* (AXT3) (Fig. 2*C*, *right*). Furthermore, alkaline pH sensitivity of KTA40-2 could not be rescued by *Arabidopsis NHX1*

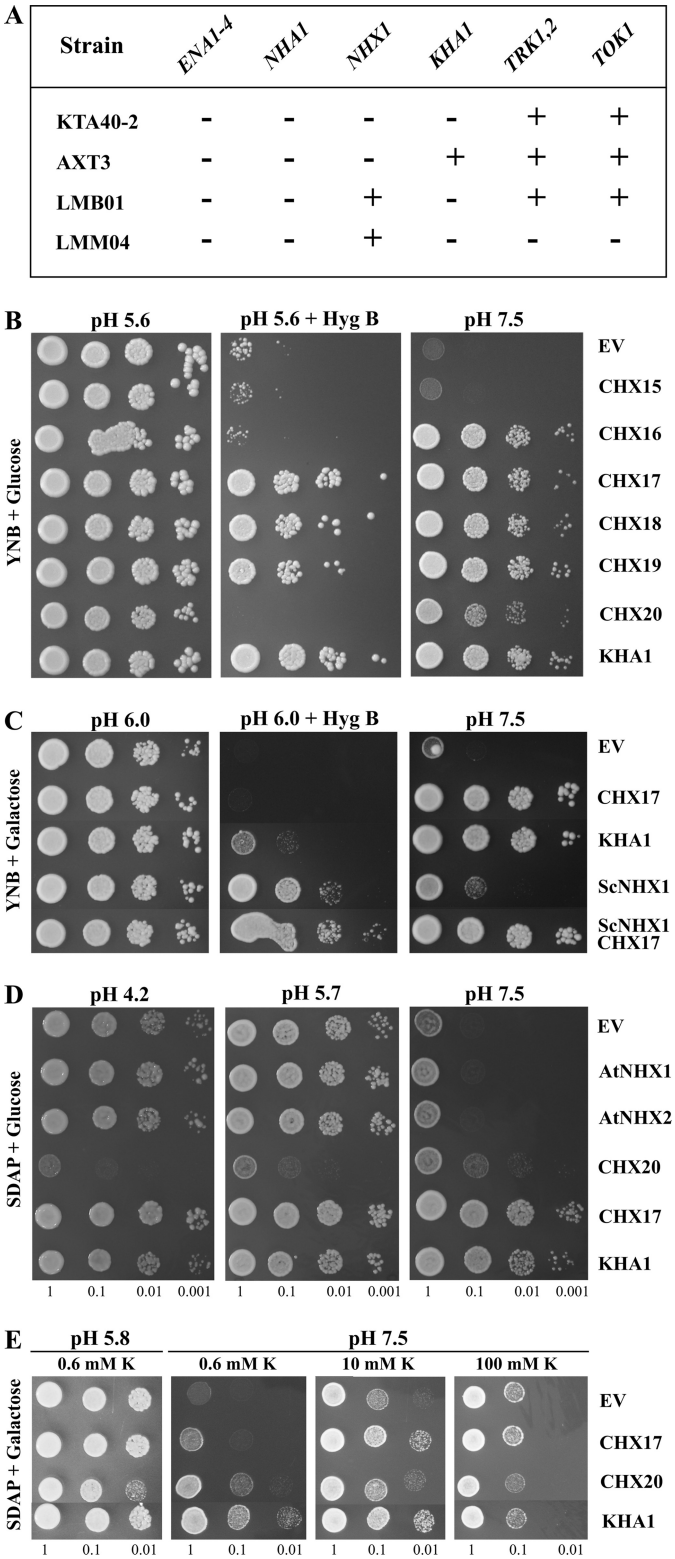

FIGURE 2. **Differential tolerance to alkaline pH and hygromycin B of yeast expressing CHXs and NHX1.** *A*, yeast strains. Wild-type or disrupted genes are denoted as + and −, respectively. Genes and corresponding proteins are *ENA1–ENA4* (PM Na^+ extrusion pumps); *NHA1* (PM Na^+/H^+ antiporter); *NHX1* (PVC Na^+/H^+ exchanger); *KHA1* (Golgi K^+/H^+ antiporter); *TRK1/2* (PM K^+ uptake pathways), and *TOK1* (a K^+ channel). *B*, differential activities. Yeast strain KTA40-2 harboring pDR196-derived empty vector (*EV*) or vector with *CHX15-CHX20* were normalized, and 5 μl of each serial dilution was dropped on medium (*far left*) at pH 5.6 or 7.5 and incubated for 3 days. *KHA1* refers to strain AXT3. Hygromycin B (*HygB*) was 100 μg/ml. *C*, pH and HygB. Yeast strain KTA40-2, AXT3, and LMB01 expressing pYES52-derived vector (*EV*) or vector with *CHX17* were prepared as above and tested at pH 6 or 7.5. *ScNHX1* refers to strain LMB01. HygB was 125 μg/ml. *D*, external pH and low K^+. Strain KTA40-2 and AXT3 expressing pDR196-derived vector (*EV*) or vector with *CHX17*, *CHX20*, *AtNHX1*, or *AtNHX2* were normalized and tested on medium with 0.6 mM K^+. *E*, wild-type strain (KHA1) or *kha1* single mutant harboring pYES52-derived vector (*EV*) or vector with *CHX17* or *CHX20* were normalized with K^+-free YNB. Cells were spotted on medium containing 0.6, 10, or 100 mM K^+ at pH 5.8 or 7.5.

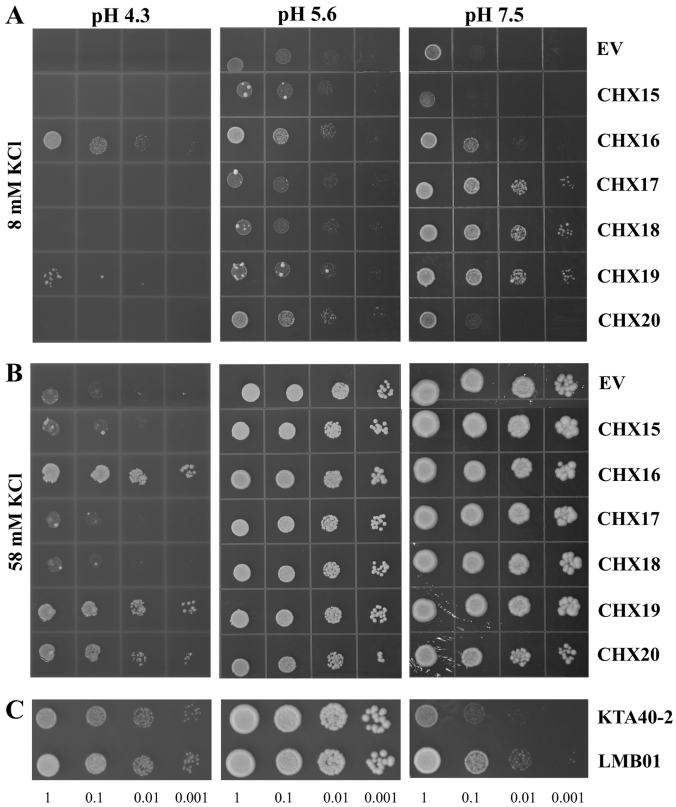

FIGURE 3. **CHX restored growth of K^+ uptake-deficient yeast depends on external [K^+] and pH.** Effect of pH and KCl at 8 mM (*A*) and 58 mM (*B*). K^+ uptake-deficient yeast strain LMM04 harboring pDR196-derived vector (*EV*) or vector with *CHX15–CHX20* was grown in YNB with 100 mM KCl and normalized. 5 μl of each serial dilution was dropped on medium at pH 4.3, 5.6, or 7.5 and incubated for 5 days. *C*, K^+ uptake-proficient strain LMB01 and KTA40-2 growing on medium with 8 mM KCl at indicated pH values after 3 days.

or *NHX2* (Fig. 2*D*). Thus, CPA2 transporters (AtCHX17 and ScKHA1) were more effective than CPA1 transporters (ScNHX1, AtNHX1, and AtNHX2) in supporting yeast growth at alkaline pH. LMB01, expressing endogenous *ScNHX1*, clearly showed stronger resistance against HygB (Fig. 2*C*, *middle*) compared with cells expressing *AtCHX17* or *ScKHA1*. Interestingly, cells expressing both *CHX17* and endogenous *ScNHX1* showed enhanced HygB resistance, suggesting an additive or cooperative effect by these two activities. These results indicate that ScKHA1 (CPA2) and ScNHX1 (CPA1) are involved in separate functions in yeast and that AtCHX17 is a functional ortholog of ScKHA1.

Growth Rescue by AtCHX16–AtCHX20 of K^+ Uptake-deficient Mutant Depends on pH_{ext}—LMM04, a K^+ uptake-deficient mutant, showed little or no growth on 8 mM K^+ (Fig. 3*A*), although growth of *TRK1/2*- and *TOK1*-positive strains (KTA40-2 and LMB01) was vigorous (Fig. 3*C*), suggesting a

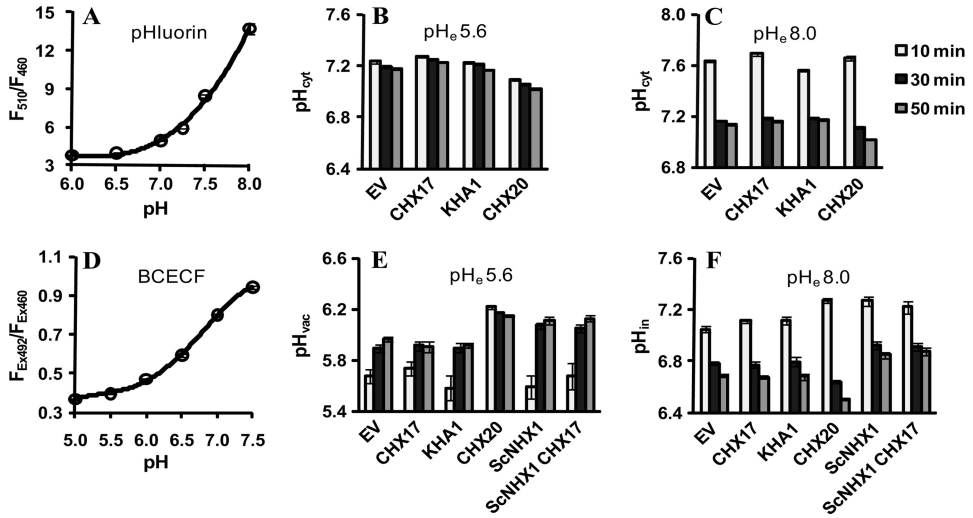

FIGURE 4. **CHX20 but not CHX17 altered cytosolic and vacuolar pH in yeast.** *A*, pH_{cell} calibration. Yeast strain KTA40-2, AXT3, and LMB01 harboring *pHluorin* in pYES52-derived vector (*EV*) or vector with CHX were added to buffers with ionophores at the indicated pH values. Results from four strains at 10, 20, and 30 min were pooled. pHluorin fluorescence (F_{510}/F_{460}) is related to pH_{cell} 6.5–8. *Bars*, S.E. ($n = 72$). *B*, pH_{ext} 5.6 on cytosolic pH. Yeast strain KTA40-2, AXT3, and LMB01 harboring *pHluorin* in empty vector (*EV*) or vector with CHX were added to K^+-free YNB with 8 mM KCl at pH 5.6. F_{510}/F_{460} was recorded at 10, 30, and 50 min. Data are from three independent lines. *Bars*, S.E. ($n = 36$). *C*, pH_{ext} 8.0 on cytosolic pH tested as in *B*. *D*, pH_{in} calibration of BCECF signals. Cells loaded with BCECF were incubated in buffers at pH 5.0–7.5 containing CCCP. Fluorescence F_{ex492}/F_{ex460} is related to *in situ* pH_{in}. Data from four strains at 20, 30, and 40 min were pooled. *Error bars*, S.E. ($n = 36$). *E*, pH_{ext} 5.6 on vacuolar pH. KTA40-2 and LMB01 carrying *ScNHX1* (*ScNHX1*) were transformed with empty vector (*EV*), *CHX17*, or *CHX20*. KHA1 refers to strain AXT3 with empty vector. Cells loaded with 50 μM BCECF were added to K^+-free YNB with 8 mM KCl at pH 5.6. Fluorescence (F_{Ex492}/F_{Ex460}) was taken at 10, 30, and 50 min. *F*, pH_{ext} 8.0 on vacuolar and intracellular pH tested as in *E*. Data are from two independent lines. *Error bars*, S.E. ($n = 12$).

crucial role of K^+ uptake in restoring growth that was optimal at pH 5.6. Intriguingly, mutants expressing *CHX17*, *CHX18*, or *CHX19* showed enhanced growth, especially at pH 7.5 (Fig. 3*A*). Furthermore, *CHX16* expression improved mutant growth partially at 8 mM $[K^+]_{ext}$ at acidic or alkaline pH values, but growth was fully restored at pH_{ext} 4.3 at 58 mM K^+ (Fig. 3*B*). However, CHX19 rescued mutant growth at pH 7.5 under 8 mM K^+ and also at pH 4.3 when K^+ was 58 mM, but it was ineffective at pH 5.6. In contrast, CHX20 enhanced growth at pH 4.3 (58 mM K^+) and 5.6 (8 mM K^+) but not at pH 7.5 (Fig. 3*A*). The differential effectiveness in supporting growth suggests that CHX17, -18, or -19 facilitated K^+ homeostasis under alkaline conditions, whereas CHX16 or CHX20 was needed under an acidic environment.

CHX17 and CHX20 Exert Differential Effects on Cytosolic and Vacuolar pH in Yeast—A pH calibration curve shows that the responsive range of pHluorin (37) is between pH 6.5 and 8.0 (Fig. 4*A*), which agrees with the apparent pK_a of 7.6 for the superecliptic pHluorin (38). Furthermore, yeast mutants co-expressing *pHluorin* and *CHX17* or *CHX20* retained their activity as shown by their ability to restore growth at alkaline pH (supplemental Fig. S2*B*).

We tested whether acidic pH_{ext} and $[K^+]_{ext}$ might alter pH_{cyt}. Basal pH_{cyt} of yeast strain AXT3 carrying the wild-type *KHA1* or KTA40-2 strain disrupted in *kha1* was estimated to be pH 7.2 after a 30-min incubation at pH 5.6 (Fig. 4*B*). Expression of *CHX17* in KTA40-2 did not significantly change pH_{cyt}. However, pH_{cyt} in the mutant expressing *CHX20* was lowered to pH 7.06, suggesting acidification resulting from activity of CHX20. When the K^+ level was lowered to 0.1 or 0.8, basal pH_{cyt} of *kha1* mutant dropped to about pH 6.9 and 7.1, respectively (supplemental Fig. S3, *A* and *C*). Expression of either *KHA1*, *CHX17*, *NHX1* (LMB01 strain), or both *NHX1* and *CHX17* did not change pH_{cyt} significantly.

After cells were exposed to alkaline pH_{ext} (Fig. 4*C*), the pH_{cyt} of all strains initially became basic (pH ~7.6); however, within 30 min, the pH_{cyt} of most strains reached a steady pH of 7.16–7.18. Similar to the acid pH shift, the mutant expressing *CHX20* showed a slightly lower pH_{cyt} of pH 7.11, which dropped to pH 7.01 after 50 min (Fig. 4*C*). However, at $[K^+]_{ext}$ of 0.1 or 0.8 mM, the pH_{cyt} dropped from ~7.4 to 7.05 and 7.15, respectively, in all strains (supplemental Fig. S3, *B* and *D*) except in mutants expressing *CHX20*, which had a pH_{cyt} of 6.88 at 50 min (supplemental Fig. S3*B*). These results indicate that (i) KHA1, CHX17, or NHX1 did not affect pH_{cyt} significantly at the external pH conditions tested; (ii) *CHX20*-expressing cells consistently acidified their pH_{cyt} by up to 0.2 units, especially when $[K^+]_{ext}$ was limiting; and (iii) adequate levels (8 mM) of K^+ seemed critical for maintaining a steady pH_{cyt} homeostasis.

Vacuolar pH was estimated using BCECF, which accumulates within yeast endosomes and vacuole (30, 39). BCECF fluorescence in H^+-permeabilized cells showed an apparent pK_a between pH 6.5 and 7.0 (Fig. 4*D*), consistent with a previous report in yeast (30). At acidic pH_{ext}, the resting pH_{vac} of strains KTA40-2 and AXT3, except for *CHX20*-expressing cells, had reached a steady pH of 5.9 after 30 min (Fig. 4*E*). Expression of *CHX17* or *KHA1* did not alter yeast pH_{vac}. However, expression of *NHX1* (LMB01 strain) significantly raised pH_{vac} to 6.1 (Fig. 4*E*) as reported previously (39). Surprisingly, expression of *CHX20* also elevated pH_{vac} to 6.13 at 50 min. Unlike cytosolic pH, vacuolar pH was slightly altered by external K^+. When K^+ was 0.1 mM, basal pH_{vac} of *kha1* mutant remained at pH ~5.9 (supplemental Fig. S3*E*). Expression of *KHA1* or *CHX17* did not significantly change pH_{vac}. Remarkably, expression of *CHX20*

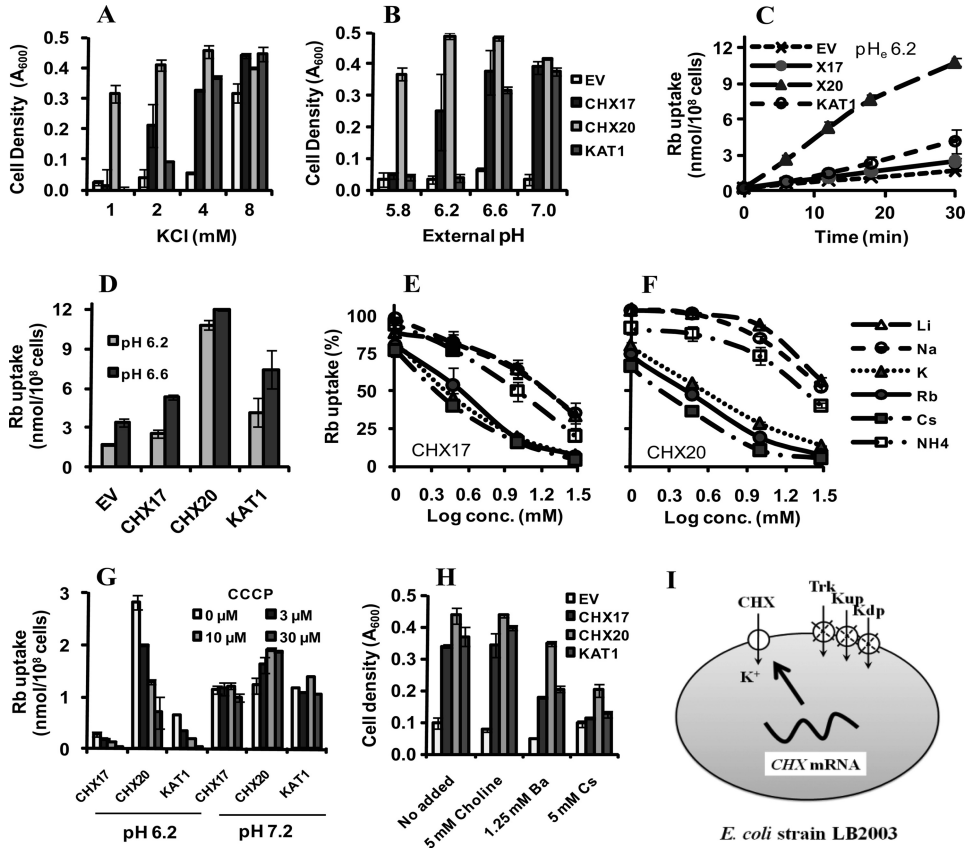

FIGURE 5. **CHX17 or CHX20 mediated K^+ uptake into *E. coli*.** *A*, cell density at varied K^+ concentration. *E. coli* strain LB2003 harboring pPAB404 vector (*EV*) or vector with *CHX17*, *CHX20*, or *KAT1* was starved for K^+ in basal SGM medium at pH 6.6 for 2 h. Cells were added to SGM-MES-MOPS medium at pH 6.6 with 1–8 mM K^+ and incubated 14 h at 30 °C. *B*, pH_{ext} on cell growth at 18 h; same as *A*, except medium contained 2 mM K^+ at varied pH values. *Error bars*, S.E. ($n = 4$). *C*, time course of Rb^+ uptake. Isopropyl β-D-thiogalactopyranoside was added to medium during K^+ starvation. Reaction mixture consisted of 2 mM RbCl at pH 6.2 and cells expressing vector (*EV*; ×) or vector harboring *CHX17* (X17; ●), *CHX20* (X20; ▲), or *KAT1* (○). An aliquot was filtered and washed at the indicated times. Data are from two independent experiments. *D*, Rb^+ uptake at pH 6.2 or 6.6. The reaction was similar to that in *C*. Uptake at 30 min is shown. *Error bars*, S.E. ($n = 2$). *E*, cations reduced CHX17-dependent Rb^+ uptake. Cells expressing *CHX17* were prepared as in *C* and normalized. The reaction mixture consisted of 0.6 mM RbCl (0.5 μCi/ml ^{86}Rb) and ~2.5×10^8 cells/ml in SGM-MES-MOPS at pH 6.2 plus one cation chloride (lithium (△), sodium (○), potassium (▲), rubidium (●), cesium (■), or NH_4 (□)) near 0, 1, 3, 10, or 30 mM. ^{86}Rb uptake was measured at 30 min. Uptake without added cation (100%) was 0.8 nmol of $Rb^+/10^8$ cells. *F*, cations on CHX20-dependent uptake. The method was the same as in *E*. Uptake without added cation (100%) was 2.4 nmol of $Rb^+/10^8$ cells. Data are from two independent experiments. *Error bars*, S.E. ($n = 2$). *G*, CCCP on Rb^+ uptake at pH 6.2 *versus* pH 7.2. Assays were similar to *C*, except cells were incubated with CCCP at 0–30 μM for 30 min. Data are from two independent experiments. Data of KAT1 are representative of three independent experiments. *Bars*, S.E. ($n = 2$). *H*, Ba^{2+} decreased *E. coli* growth supported by CHX17 or KAT1. Cells expressing vector only or *CHX17*, *CHX20*, or *KAT1* were incubated in medium containing 5 mM K^+ at pH 6.6 plus 5 mM choline chloride, 1.25 mM $BaCl_2$, or 5 mM CsCl for 18 h. *Error bars*, S.E. ($n = 4$). *I*, rescue of mutations in three K^+ uptake transport systems, Trk, Kup, and Kdp, in *E. coli* LB2003 by exogenous *Arabidopsis* CHX transporters.

further alkalinized pH_{vac} to 6.28 (supplemental Fig. S3*E*), but this alkalinization was reduced in strain LMB01, as observed by pH_{vac} 6.03 at limiting K^+ concentration.

In alkaline medium, BCECF signal reflects the average intracellular pH (pH_{in}) because the dye was localized at both cytosol and vacuole. The pH_{in} of cells expressing *CHX17* or *KHA1* was pH 7.1 initially but dropped to 6.6 after 1 h. However, expression of *NHX1* resulted in a pH_{in} of 0.2 units higher. Because these strains maintained a similar pH_{cyt} (Fig. 4*C* and supplemental Fig. S3, *B* and *D*), the results imply that only NHX1 alkalinized pH_{vac}. The role of CHX20 in yeast is less certain because it altered both pH_{cyt} and pH_{vac}. These results showed that CHX17 or KHA1 had no effect on regulating bulk vacuolar pH when pH_{ext} was either acidic or alkaline.

Together, the ability of CHX17 or KHA1 to confer yeast growth tolerance on alkaline medium was not accompanied by alteration of bulk cytosolic pH or vacuolar pH. NHX1 did alkalinize vacuolar pH, consistent with prior reports (29, 39). *CHX20*, however, differed because cells expressing this gene consistently showed a more acidic pH_{cyt} and a more basic pH_{vac}.

CHX17-mediated K^+ Uptake in E. coli—We were unable to detect significant changes in K^+ ($^{86}Rb^+$) fluxes resulting from expression of *CHX17* or *CHX20* in yeast LMM04 cells at either pH 7.5 or pH 4.5 (supplemental Fig. S4); therefore, we expressed *CHX17* and *CHX20* in *E. coli* strain LB2003 that is defective in three K^+ uptake systems (25). In this system, heterologously expressed membrane protein would be inserted in the plasma membrane (40). Both CHX17 and CHX20 restored bacterial growth on YTM medium containing 1–4 mM K^+ at pH 6.6 (supplemental Fig. S5*A*). Increasing concentrations of K^+ and Rb^+, but not Na^+, enhanced growth of cells harboring CHX17, CHX20, or KAT1 at pH 5.5 (supplemental Fig. S5*B*), indicating that Rb^+ can partially substitute for K^+. KAT1 is an inward rectifying K^+ channel from *Arabidopsis* (41) and serves as a positive control.

Using SGM medium to better control K^+ levels, we showed that CHX17 restored growth of LB2003 strain at 2–4 mM K^+, similar to KAT1. CHX20 was more effective because it increased bacterial growth at 1 mM K^+ (Fig. 5*A*). By 8 mM K^+, cells harboring empty vector grew as fast as others, indicating that K^+ is taken up via nonspecific pathways. CHX20 rescued bacteria growth at all pH values tested (Fig. 5*B*), although CHX17- or KAT1-enhanced growth was nearly optimal at pH 7.0. These results indicate that growth rescue by CHX17 and CHX20 is influenced differently by external K^+ and pH.

CHX20 mediated $^{86}Rb^+$ uptake at a faster rate than that facilitated by CHX17 or KAT1 at pH 6.2 and 6.6 (Fig. 5, *C* and *D*). We chose pH 6.2 for further experiments to minimize nonspecific Rb influx. These results demonstrated that CHX17 and CHX20 mediated K^+ uptake in a pH-dependent manner. K^+ or Rb^+ reduced CHX17-dependent ^{86}Rb uptake with an IC_{50} (half-maximal inhibitory concentration) of about 2.6 mM, relative to an IC_{50} of 17–36 mM by Li^+ or Na^+ (Fig. 5, *E* and *F*, and supplemental Fig. S10). The concentration of Cs^+, Rb^+, and K^+ required to inhibit CHX20-dependent Rb^+ flux (IC_{50}) was 1.5, 2.5, and 3.8 mM, respectively, indicating that CHX20 preferred $Cs^+ > Rb^+ > K^+$. KAT1 also showed a slight preference of K^+ over Rb^+ (supplemental Fig. S10) based on the IC_{50} of 2.1 and 3.2 mM, respectively, consistent with the study by Uozumi *et al.* (42). Thus, CHX17 and CHX20 are monovalent cation transporters with an apparent K_m for K^+ in the low millimolar range.

CCCP decreased Rb^+ uptake mediated by CHX17, CHX20, and KAT1 (Fig. 5*G*) at pH 6.2. Curiously, an increase in Rb^+ uptake in cells harboring CHX20 was observed at pH 7.2 in the presence of CCCP. However, CCCP caused no change in Rb uptake mediated by CHX17 or KAT1. This result would suggest that CHX20-mediated K^+ transpot is coupled to a pH gradient, whereas CHX17-dependent K^+ transport is not. Ba^{2+} at 1.25 mM reduced *E. coli* growth dependent on CHX17 or KAT1 by 50% relative to the control but reduced growth of cells harboring CHX20 by only 20% (Fig. 5*H*). Moreover, Cs^+ at 5 mM inhibited CHX17- or KAT1-dependent growth more than that of cells harboring CHX20. Thus, the mode of K^+ transport mediated by CHX17 might differ from that of CHX20.

Localization of CHXs to Endomembrane in Yeast and in Plant Cells—All CHXs tagged at the carboxyl end to GFP were shown to restore growth of KTA40-2 mutants on alkaline medium (supplemental Fig. S6). Furthermore, resistance to HygB was also retained in cells expressing GFP-tagged *CHX17*, *CHX18*, or *CHX19*. Cells expressing *CHX16*-GFP or *CHX20*-GFP were hypersensitive to HygB (supplemental Fig. S6, *middle*), as shown before for the untagged protein (Fig. 2*B*). These results demonstrate that CHX16–CHX20 tagged at the C-terminal end with GFP retained their native activity.

In wild-type yeast (FY833), CHX17-GFP and CHX20-GFP fluorescence appeared on tubular and reticulate structures (Fig. 6*A*). The GFP signal co-localized poorly with that of FM4-64 (Fig. 6*A*), indicating that CHX17 or CHX20 proteins were not associated with the PM, endosomes, or vacuole. These patterns suggested that CHX17 and CHX20 were localized to distinct endomembranes. In contrast, AtNHX1-GFP labeled intracellular membranes that were mainly reticulate and partially overlapped with FM4-64.

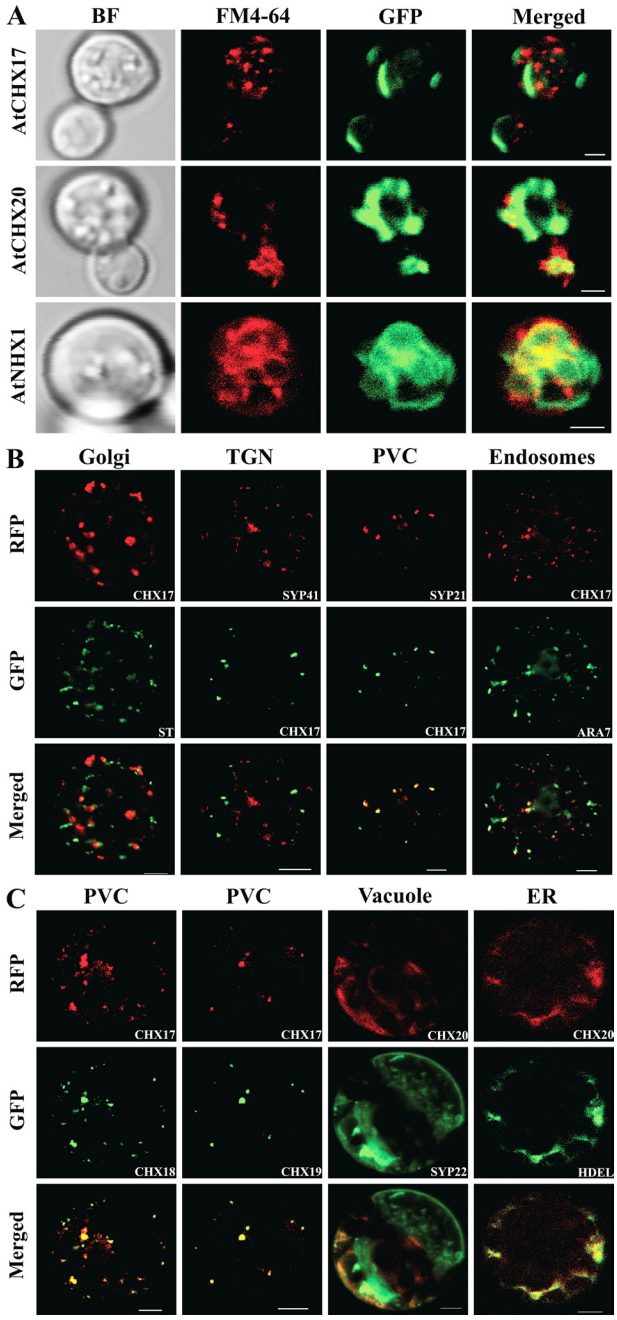

FIGURE 6. **Differential localization of CHX17-CHX20 in endomembranes.** *A*, distribution of AtNHX1, CHX17, CHX20, and FM4-64 in yeast. WT strain FY833 harboring *CHX17*, *CHX20*, or *AtNHX1* fused with GFP at the C terminus was grown in YNB, transferred to YPAD medium, and incubated for 4 h. Cells were observed after 10 min in 10 μM FM4-64. The *merged column* shows images of GFP-labeled (*column 1*) and FM4-64-labeled (*column 2*) cells shown in bright field (*right*). *Bar*, 2 μm. *B*, CHX17 localized to PVC. Plant protoplasts were co-transfected with *CHX17*-GFP or *CHX17*-RFP and a tagged marker. Markers used were Golgi ST-GFP, *trans*-Golgi network RFP-SYP41, PVC RFP-SYP21, and endosomes GFP-ARA7. Signals were observed at 18–24 h. *Merged signals* from GFP and RFP are shown in the *bottom row*. *Bars*, 5 μm. *C*, CHX18 and CHX19 localized to PVC, whereas CHX20 localized to ER. Protoplasts were co-transfected with *CHX18*-GFP, *CHX19*-GFP, or *CHX20*-RFP and a marker as in *B*. CHX17-RFP, Syp22-GFP, and HDEL-GFP served as markers for PVC, vacuole, and ER, respectively. *Bars*, 5 μm.

In plant cells, CHX17-GFP alone showed a punctate pattern (supplemental Fig. S7). CHX17 did not co-localize with sialyltransferase or syntaxin 41, suggesting that CHX17 was not associated with the Golgi or the *trans*-Golgi network. However,

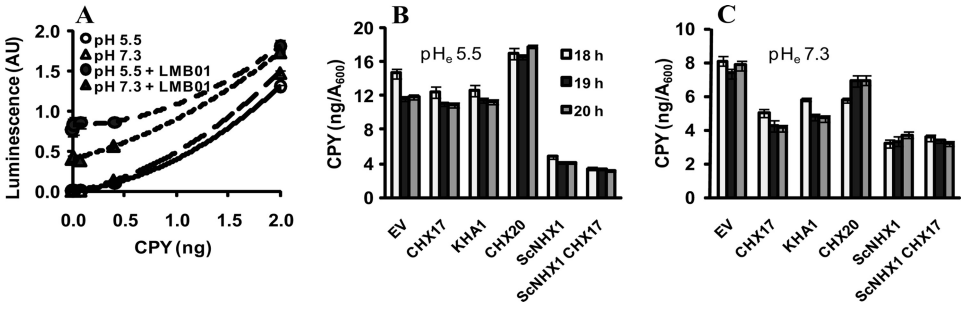

FIGURE 7. **CHX17 reduced extracellular carboxypeptidase Y in yeast at alkaline pH.** *A*, standard CPY. Purified CPY at the indicated amount (ng) was added to an ELISA plate with or without yeast strain LMB01 at pH 5.5 (●, ○) or 7.3 (▲, △). After 20 h, cells were removed, and CPY was detected by immunoassay. *AU*, arbitrary unit. *Error bars*, S.E. ($n = 14$). *B*, extracellular CPY of yeast at pH_{ext} 5.5. Yeast strain KTA40-2, AXT3, and LMB01 (Fig. 2*A*) were transformed with pYES52-derived plasmid alone (*EV*) or vector with *CHX17* or *CHX20*. *KHA1* and *ScNHX1* refer to strain AXT3 and LMB01, respectively. Yeast was grown in YNB, normalized to A_{600} of 0.2, and added to K^+-free YNB with 2% galactose and 8 mM K^+ at pH 5.5. CPY on plate was detected at early log phase (18–20 h). Signals were normalized to cell density (A_{600}) and converted to ng of CPY/A_{600} cells. Data are from seven replicates of two independent lines. *Error bars*, S.E. ($n = 14$). *C*, extracellular CPY of cells grown at pH 7.3. The experiment was conducted as in *B*, except the initial A_{600} was 0.8 and pH of the medium was 7.3. *Error bars*, S.E. ($n = 14$).

CHX17 co-localized very well with syntaxin 21 and partially with RabF2b or Ara7 (Fig. 6*B*), suggesting that CHX17 was in prevacuolar compartments (PVC), a subset of endosomes. Moreover, CHX18 and CHX19 co-localized with CHX17, suggesting that these two proteins were also at the PVC (Fig. 6*C*). In contrast, CHX20-RFP gave a reticulate pattern that co-localized with an ER marker (GFP-HDEL) but not with syntaxin 22 (Fig. 6*C*). In addition, CHX16-GFP showed a reticulate pattern (supplemental Fig. S7), implying that CHX16 and CHX20 were associated with ER.

CHX17 or CHX20 Altered Efficiency of CPY Sorting Depending on pH_{ext}—We tested if CHX17 or CHX20 had a role in protein sorting. Carboxypeptidase Y (CPY) is normally trafficked from Golgi to the vacuole lumen via the prevacuolar/late endosomal compartment in yeast. Cells with the same density were cultured in medium at pH 5.7 or 7.3, and growth was monitored continuously using A_{600} (supplemental Fig. S8). Extracellular CPY was determined and normalized to cell density. The assay was validated with purified yeast CPY with or without yeast cells (LMB01) at pH 5.5 or pH 7.3. pH_{ext} had little to no effect on CPY detection without yeast cells (Fig. 7*A*). Yeasts grown at pH 5.5 showed more CPY in the medium than cells grown at pH 7.3 (Fig. 7*A*). This result shows that immunodetected CPY in the medium is related with extracellular CPY in the medium.

Similar levels of extracellular CPY were detected in KTA40-2 mutants expressing empty vector (11.8 ng/A_{600}), *CHX17* (11.0 ng/A_{600}) or *KHA1* (11.3 ng/A_{600}) at pH 5.5 (Fig. 7*B*). However, strains expressing *NHX1* (LMB01) alone or *NHX1* and *CHX17* showed minimal extracellular CPY (4.0 and 3.3 ng/A_{600}), supporting prior findings that NHX1 is critical for sorting proteins to the vacuole (43, 44). Thus, CHX17 has little or no additional effect when NHX1 is present in cells growing in acidic medium. However, CHX20 resulted in enhanced secretion of CPY, indicating a perturbation of CPY trafficking.

At alkaline pH_{ext}, mutants expressing *CHX17* or *KHA1* showed reduced extracellular CPY (4.1 or 4.7 ng/A_{600}), relative to 7.8 ng/A_{600} of the KTA40-2 mutant (Fig. 7*C*). Expression of *NHX1* with or without *CHX17* (in LMB01 cells) also decreased CPY levels (3.7 or 3.2 ng/A_{600}). These results would suggest that protein sorting and membrane trafficking pattern are shifted in KTA40-2 mutants expressing *CHX17* or *KHA1*, resulting in reduced secretion in cells grown at alkaline pH. Thus, CHX17 or KHA1 are effective in altering trafficking patterns in cells in a pH-dependent manner. Curiously, cells expressing *CHX20* did not show a similar reduction in CPY secretion levels at alkaline pH_{ext}, suggesting that it may influence protein sorting in a differential manner.

DISCUSSION

Tolerance to Alkaline pH: Diversity among Five CHXs—For years, it had been challenging to determine CHX gene functions because they failed to restore growth in various yeast mutants. A striking phenotype of *AtCHX16–AtCHX20* expressed in KTA40-2 yeast mutant is their ability to restore growth at alkaline pH. This breakthrough was made initially using AtCHX20 (21) and AtCHX17 (24), although the mechanistic basis was unknown. Without any obvious working hypothesis, we have first compared properties of five CHXs with NHX1. Here we show that *Arabidopsis* CHX17, -18, or -19 is most effective in conferring tolerance to alkaline pH of KTA40-2 mutants, similar to yeast KHA1. By contrast, CHX20 or CHX16 is less effective in conferring alkaline tolerance. Furthermore, cells expressing *CHX17*, *-18*, and *-19* were resistant to hygromycin B, whereas cells expressing *CHX16* or *CHX20* were sensitive or hypersensitive. Importantly, the properties of CHX17 differed from those of ScNHX1 or AtNHX1. ScNHX1 was unable to restore growth of KTA40-2 mutant at alkaline pH and was more effective in conferring HygB resistance than CHX17, as seen between ScNHX1 and ScKHA1 (45). The variations observed among five AtCHXs cannot be attributed to unequivalent expression of protein levels because (i) the qualitative phenotypes are consistently observed in independent transformants, (ii) GFP-tagged CHX16 through CHX20 at the C terminus are active in conferring alkaline tolerance and are localized to intracellular membranes in yeast, and (iii) CHX17-GFP conferred HygB resistance, whereas CHX20-GFP or CHX16-GFP did not. Thus, all five CHX proteins (CHX16–CHX20) appear to function in pH homeostasis in yeast in a manner distinct from NHX1. Moreover, CHX17, CHX18, and CHX19 diverge in activity from CHX16 and CHX20.

Importance of K^+ in pH Homeostasis—Several observations pointed to a role of $[K^+]_{ext}$ in pH homeostasis and in growth of yeast mutants expressing CHX: (i) CHX17- or CHX20-enhanced growth of single *kha1* mutant at alkaline pH was evident at 0.6–10 mM $[K^+]$ but not at 100 mM (Fig. 2*E*); (ii) CHX17–CHX19 restored growth of K^+ uptake-deficient mutant LMM04 at pH 7.5, similar to yeast harboring K^+ uptake systems, Trk1/2 and Tok1 (Fig. 3, *A* and *C*); and (iii) CHX16, CHX19, and CHX20 restored growth at pH 4.3 (Fig. 3*B*). The increased growth of K^+ uptake-deficient mutants by CHX17, -18, or -19 at alkaline pH would suggest that intracellular K^+ is needed for growth and that these CHXs facilitated K^+ acquisition into cells. However, there was no increase in K^+ ($^{86}Rb^+$) flux at pH 7.5 or pH 4.5 into K^+ uptake-deficient yeast (LMM04) expressing *CHX17* (supplemental Fig. S4, *A* and *B*). Curiously, KTA40-2 strains expressing *CHX17* or *CHX20* took up less K^+ than in mutants with vector only, and cells grown at pH 7.5 took up 3-fold more K^+ than at pH 4.5 (supplemental Fig. S4, *C* and *D*). Because both CHX17 and CHX20 were localized to endomembranes in yeast, these results suggest that both CHX proteins do not enhance net K^+ uptake into cells but rather are important in cation uptake, K^+ sorting and/or cycling through certain endomembrane compartments and the cell. This interpretation could also apply to yeast ScKHA1, which has been localized to Golgi (24, 46).

CHX17- and CHX20-mediated K^+ Transport—Here we provide the first functional characterization of CHX17- and CHX20-mediated K^+ transport using a K^+ uptake-deficient *E. coli* strain (Fig. 5*I*). CHX20 enhanced *E. coli* LB2003 growth at acidic pH (pH 5.8–6.2), whereas cells expressing CHX17 or KAT1 showed optimal growth at pH 6.6–7. Cation competition studies showed that CHX17 preferred $K^+ = Rb^+ > Na^+$, whereas CHX20 showed specificity for $Cs^+ > Rb^+ > K^+ \gg Na^+$. Thus, K^+ is the physiological substrate, and both CHX17 and CHX20 transport K^+ with a K_m in the low millimolar range. Cs^+ blocked Rb^+ flux; this may be due to CHX20-mediated Cs^+ transport because the Cs^+ accumulation trait was mapped to the *AtCHX20* locus using the quantitative trait loci method (47). Thus, CHX17 and CHX20 are monovalent cation transporters with distinct properties, although their mode of transport and relationship to pH homeostasis is unclear (see below).

Several observations suggested that CHX20 mediated H^+-coupled K^+ transport: (i) K^+ influx into *E. coli* is optimal when pH_{ext} is acidic, and (ii) CCCP, a protonophore, inhibited K^+ uptake at pH 6.2 but not at pH_{ext} 7.2, when there is little or no pH gradient across the PM. However, at pH 7.2, increasing CCCP concentration enhanced CHX20-dependent Rb^+ uptake into cells. This finding is surprising, unless the protein has switched its mode of transport.

Transport properties of CHX17 mimicked that of KAT1, an inwardly rectifying K^+ channel. They both showed optimal transport near neutral pH, and K^+ influx was insensitive to the protonophore CCCP at neutral pH. Bacterial growth stimulated by both CHX17 and KAT1 is inhibited ~50% by 1.25 mM Ba^{2+}, a K^+ channel blocker (41, 48), whereas CHX20-supported growth is less sensitive. It is possible that CHX20 behaves like a H^+-coupled K^+ symporter and CHX17 has channel-like properties, although this idea will need to be rigorously verified. Interestingly, examples are emerging where channel properties exist in transporters (49). For example, KefC (a homolog of AtKEA1/2) has channel-like properties and cation/proton antiport activity when co-expressed with a peripheral protein, KefF (50). Despite the ambiguity, we postulate that K^+ transport mediated by CHX is probably coupled either directly or indirectly to a H^+ flux, which would change compartment pH or localized pH at an endomembrane.

Differential Effects of CHX17 and CHX20 on Intracellular pH—The inability to detect changes in cytosolic or vacuolar pH in yeast expressing *CHX17* or *ScKHA1* could be due to the relatively weak or limited signal from small compartments. In contrast, pH changes in vacuoles were detected because cells expressing *NHX1* had a slightly basic pH in vacuoles (pH 6.1) relative to pH 5.9 of vacuoles in KTA40-2 (*nhx1*Δ) (Fig. 4*E*). Our results are consistent with the model that NHX1 alkalinizes vacuolar pH (29).

Furthermore, cells expressing *CHX20* alkalinized the vacuole and acidified the cytosol by about 0.2 units, indicating that the roles of CHX20 differed from that of CHX17. At limiting K^+ (0.1 mM; supplemental Fig. S3*E*) pH_{vac} increased from 5.92 to 6.28 (~0.4 units) in cells expressing *CHX20*, whereas *NHX1* alkalinized pH_{vac} by about 0.1 unit to pH 6.03. This result suggested that CHX20 and NHX1 show differential modes of transport. It was shown before that vacuolar K^+ concentration changed according to K^+ availability in the tissue (51). If so, K^+ transport into the vacuole via NHX1-mediated electroneutral K^+/H^+ exchange would be reduced at low K^+; however, the increase in vacuolar alkalinization and cytosolic acidification seen in cells with CHX20 would favor a model of a H^+/K^+ symporter (see above).

These results would suggest that tolerance to alkaline pH conferred by either CHX17 or CHX20 was not due largely to changes in pH_{cyt} or pH_{vac}. Instead, altered pH in cells expressing *CHX20* could be related to HygB sensitivity and compromised growth at pH 4.2 (Fig. 2*D*).

Endosomal pH, Protein Sorting, and Membrane Trafficking—Our results point to roles of CHX16–CHX20 transporters in protein sorting and membrane trafficking. First, it is well known that yeast mutants sensitive to alkaline pH are defective in genes important for endomembrane acidification, vacuolar protein sorting, or vacuole biogenesis (52). For instance, *vma* mutants with defects in H^+-pumping V-ATPase subunits fail to grow at pH 7.5 but proliferate normally on medium at pH 5.5 (53), as long as the endolumenal compartments are acidic (30). Thus, perturbing acidification of the endolumenal compartment reduces cell proliferation. Here we showed that the growth sensitivity to alkaline pH of *kha1* mutant is reversed at acidic pH_{ext} (Fig. 2*E*), similar to *vma* mutants. Moreover, we demonstrated that growth of *kha1* mutant or KTA40-2 was rescued at alkaline pH by CHX17 or KHA1. Thus, our results suggest that CHX17 or KHA1 is involved in adjusting cation and pH of one or more endomembrane compartments and thus enhance cell proliferation.

Second, yeast mutant KTA40-2 lacking several endomembrane cation/H^+ exchangers secreted vacuolar CPY; however, mutants expressing *CHX17* or *CHX20* secreted less CPY at pH 7.3 (37–39%) relative to that seen at pH 5.5 (Fig. 7, *B* and *C*).

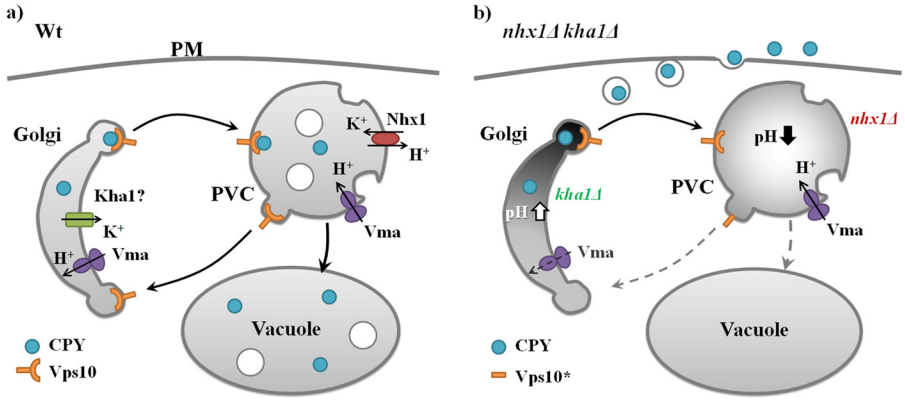

FIGURE 8. **Roles of ScNHX1, ScKHA1, and AtCHX17 in membrane trafficking and protein sorting in yeast.** *a*, in wild type (*Wt*), CPY is synthesized at the ER, processed at the Golgi, and sorted to the PVC by the vacuolar sorting receptor (Vps10), which cycles between late Golgi and PVC. CPY is then delivered to the vacuole. *b*, in the *nhx1*Δ mutant, PVC is acidified (29), leading to degradation of Vps10*, so CPY in late Golgi is secreted instead (44). In the *nhx1*Δ *kha1*Δ double mutant, it is postulated that lumenal pH and K^+ balance in PVC and Golgi (46) are altered, thereby enhancing CPY secretion. AtCHX17 appears to serve a role similar to ScKHA1 in yeast.

Like *CHX17*, *ScKHA1* expression also reduced CPY secretion (52–60%) relative to KTA40-2 mutant alone at alkaline pH. In contrast, ScNHX1 reduced CPY secretion in LMB01 yeast at both acidic and alkaline pH. Our results are consistent with previous work demonstrating that pH modulation of endosome/PVC by ScNHX1 (29) is important for trafficking of vacuolar sorting receptor, Vps10, which normally binds and sorts CPY from Golgi to vacuole (39, 44) (Fig. 8). Because CHX17 (Fig. 6) and ScKHA1 (24, 46) were localized to endomembranes, we propose a model where modulation of cation and pH homeostasis in ER, Golgi, and/or related compartments is critical for proper protein sorting and membrane trafficking. CHX17 could serve a similar model in endosomes/PVC of plant cells.

Third, the ability of CHX17 and ScNHX1 to confer hygromycin B resistance in yeast could be related to vesicle trafficking. The cellular basis of aminoglycoside resistance in yeast is still debatable. Toxicity has been attributed to the extent of hygromycin B transport into the cytosol, where it binds the 30 S ribosome and blocks protein translation (54). Yeasts grown under K^+-starved condition are sensitive, suggesting an increase in potential-driven uptake of $HygB^+$ (35), yet *kha1* or *nhx1* mutants showed no change in membrane potential (55, 56). One study showed that gentamicin, another aminoglycoside, enters pig kidney cells (LLC-PK1) via endocytosis and is then delivered by retrograde traffic to the lysosome and ER/Golgi, where its leakage into the cytosol poisons the cell (57). Furthermore, several gentamicin-sensitive yeast mutants are defective in genes associated with the Golgi-associated retrograde pathway or homotypic fusion and vacuolar protein sorting (58). Thus, gentamicin sensitivity in yeast is related to altered intracellular membrane trafficking. We found that CHX17, KHA1, or NHX1 conferred both HygB and gentamicin resistance (supplemental Fig. S9). Some mutants of *vma*, *vps*, or *pep* genes are also sensitive to HygB. Because Vps44 or NHX1 alkalinizes the vacuole (29) and confers tolerance to HygB or gentamicin, we propose that NHX1 could influence sorting of the antibiotic into a compartment (*e.g.* vacuole) for degradation or inactivation. CHX17 confers an additive effect of HygB resistance on cells harboring wild-type NHX1 (Fig. 2*B*), suggesting that CHX17 also modulated pH or cation balance of compartments that collaborate to facilitate retrograde transport, leading to degradation or inactivation of the antibiotic. Furthermore, the inability of CHX20 to confer HygB resistance could be attributed to its different transport properties, its association with distinct endomembranes, or both, which would interfere with antibiotic sorting and inactivation.

Summary—This study has revealed distinct properties of two *Arabidopsis* K^+ transporters, CHX17 and CHX20, after expression in yeast and *E. coli*. Our findings point to a common role of CHXs in modulating cation and pH homeostasis of diverse endosomal compartments. Apart from the role of CHX20 in guard cell movement, phenotypic analyses of single or high order mutants of CHX16 through CHX19 have been unremarkable so far. Mutant *chx17* plants grown under K^+ starvation showed reduced K^+ content, supporting a role in K^+ homeostasis (23). Increased expression of *CHX17* transcripts by K^+ starvation, abscisic acid, or high salt (23) would suggest additional roles in stress tolerance. Our finding that endosome-associated CHX17 alters vacuolar CPY sorting in yeast supports a role in membrane trafficking. Whether it influences the anterograde or retrograde trafficking among ER, PVC, and endosomes has yet to be established. It is clear that NHX1 and CHX17 functions can partially overlap yet are distinct in yeast and possibly in plants. Together, our studies provide the first indication that members of the CHX family are monovalent cation transporters with distinct and critical roles in membrane trafficking that would impact stress tolerance, development, and growth of plants.

Acknowledgments—We thank Drs. Chunxin Wang, Alex Bao, Quansheng Qui, and Dorothy Belle Poli (University of Maryland) for conducting preliminary studies on the CHX gene family and Lalu Zulkifli (Tohoku University) for initial studies using E. coli. Jose Pardo (Instituto de Recursos Naturales y Agrobiologia-Consejo Superior de Investigaciones Científicas) provided AtNHX1-GFP plasmid.

REFERENCES

1. Jurgens, G. (2004) *Annu. Rev. Cell Dev. Biol.* **20,** 481–504
2. Orlowski, J., and Grinstein, S. (2007) *Curr. Opin. Cell Biol.* **19,** 483–492
3. Casey, J. R., Grinstein, S., and Orlowski, J. (2010) *Nat. Rev. Mol. Cell Biol.*

11, 50–61
4. Rose, J. K., and Lee, S. J. (2010) *Plant Physiol.* **153,** 433–436
5. Kane, P. M. (2006) *Microbiol. Mol. Biol. Rev.* **70,** 177–191
6. Sze, H., Ward, J. M., and Lai, S. (1992) *J. Bioenerg. Biomembr.* **24,** 371–381
7. Schumacher, K., and Krebs, M. (2010) *Curr. Opin. Plant Biol.* **13,** 724–730
8. Nishi, T., and Forgac, M. (2002) *Nat. Rev. Mol. Cell Biol.* **3,** 94–103
9. Sze, H. (1985) *Annu. Rev. Plant Physiol.* **36,** 175–208
10. Brett, C. L., Donowitz, M., and Rao, R. (2005) *Am. J. Physiol. Cell Physiol.* **288,** C223–C239
11. Pardo, J. M., Cubero, B., Leidi, E. O., and Quintero, F. J. (2006) *J. Exp. Bot* **57,** 1181–1199
12. Gaxiola, R. A., Rao, R., Sherman, A., Grisafi, P., Alper, S. L., and Fink, G. R. (1999) *Proc. Natl. Acad. Sci. U.S.A.* **96,** 1480–1485
13. Apse, M. P., Aharon, G. S., Snedden, W. A., and Blumwald, E. (1999) *Science* **285,** 1256–1258
14. Venema, K., Quintero, F. J., Pardo, J. M., and Donaire, J. P. (2002) *J. Biol. Chem.* **277,** 2413–2418
15. Venema, K., Belver, A., Marin-Manzano, M. C., Rodríguez-Rosales, M. P., and Donaire, J. P. (2003) *J. Biol. Chem.* **278,** 22453–22459
16. Bassil, E., Ohto, M. A., Esumi, T., Tajima, H., Zhu, Z., Cagnac, O., Belmonte, M., Peleg, Z., Yamaguchi, T., and Blumwald, E. (2011) *Plant Cell* **23,** 224–239
17. Shi, H., Quintero, F. J., Pardo, J. M., and Zhu, J. K. (2002) *Plant Cell* **14,** 465–477
18. Sze, H., Padmanaban, S., Cellier, F., Honys, D., Cheng, N. H., Bock, K. W., Conéjéro, G., Li, X., Twell, D., Ward, J. M., and Hirschi, K. D. (2004) *Plant Physiol.* **136,** 2532–2547
19. Xiang, M., Feng, M., Muend, S., and Rao, R. (2007) *Proc. Natl. Acad. Sci. U.S.A.* **104,** 18677–18681
20. Bock, K. W., Honys, D., Ward, J. M., Padmanaban, S., Nawrocki, E. P., Hirschi, K. D., Twell, D., and Sze, H. (2006) *Plant Physiol.* **140,** 1151–1168
21. Padmanaban, S., Chanroj, S., Kwak, J. M., Li, X., Ward, J. M., and Sze, H. (2007) *Plant Physiol.* **144,** 82–93
22. Lu, Y., Chanroj, S., Zulkifli, L., Johnson, M. A., Uozumi, N., Cheung, A., and Sze, H. (2011) *Plant Cell* **23,** 81–93
23. Cellier, F., Conéjéro, G., Ricaud, L., Luu, D. T., Lepetit, M., Gosti, F., and Casse, F. (2004) *Plant J.* **39,** 834–846
24. Maresova, L., and Sychrova, H. (2006) *Yeast* **23,** 1167–1171
25. Stumpe, S., and Bakker, E. P. (1997) *Arch. Microbiol.* **167,** 126–136
26. Buurman, E. T., Kim, K. T., and Epstein, W. (1995) *J. Biol. Chem.* **270,** 6678–6685
27. Gietz, R. D., and Schiestl, R. H. (2007) *Nat. Protoc.* **2,** 1–4
28. Oldenburg, K. R., Vo, K. T., Michaelis, S., and Paddon, C. (1997) *Nucleic Acids Res.* **25,** 451–452
29. Brett, C. L., Tukaye, D. N., Mukherjee, S., and Rao, R. (2005) *Mol. Biol. Cell* **16,** 1396–1405
30. Plant, P. J., Manolson, M. F., Grinstein, S., and Demaurex, N. (1999) *J. Biol. Chem.* **274,** 37270–37279
31. Uozumi, N., Nakamura, T., Schroeder, J. I., and Muto, S. (1998) *Proc. Natl. Acad. Sci. U.S.A.* **95,** 9773–9778
32. Tsunekawa, K., Shijuku, T., Hayashimoto, M., Kojima, Y., Onai, K., Morishita, M., Ishiura, M., Kuroda, T., Nakamura, T., Kobayashi, H., Sato, M., Toyooka, K., Matsuoka, K., Omata, T., and Uozumi, N. (2009) *J. Biol. Chem.* **284,** 16513–16521
33. Li, X., Chanroj, S., Wu, Z., Romanowsky, S. M., Harper, J. F., and Sze, H. (2008) *Plant Physiol.* **147,** 1675–1689
34. Yoo, S. D., Cho, Y. H., and Sheen, J. (2007) *Nat. Protoc.* **2,** 1565–1572
35. Perlin, D. S., Brown, C. L., and Haber, J. E. (1988) *J. Biol. Chem.* **263,** 18118–18122
36. Banuelos, M. G., Moreno, D. E., Olson, D. K., Nguyen, Q., Ricarte, F., Aguilera-Sandoval, C. R., and Gharakhanian, E. (2010) *Curr. Genet.* **56,** 121–137
37. Miesenböck, G., De Angelis, D. A., and Rothman, J. E. (1998) *Nature* **394,** 192–195
38. Schulte, A., Lorenzen, I., Böttcher, M., and Plieth, C. (2006) *Plant Methods* **2,** 7
39. Ali, R., Brett, C. L., Mukherjee, S., and Rao, R. (2004) *J. Biol. Chem.* **279,** 4498–4506
40. Uozumi, N. (2001) *Am. J. Physiol. Cell Physiol.* **281,** C733–C739
41. Schachtman, D. P., Schroeder, J. I., Lucas, W. J., Anderson, J. A., and Gaber, R. F. (1992) *Science* **258,** 1654–1658
42. Uozumi, N., Gassmann, W., Cao, Y., and Schroeder, J. I. (1995) *J. Biol. Chem.* **270,** 24276–24281
43. Mukherjee, S., Kallay, L., Brett, C. L., and Rao, R. (2006) *Biochem. J.* **398,** 97–105
44. Bowers, K., Levi, B. P., Patel, F. I., and Stevens, T. H. (2000) *Mol. Biol. Cell* **11,** 4277–4294
45. Maresova, L., and Sychrova, H. (2005) *Mol. Microbiol.* **55,** 588–600
46. Flis, K., Hinzpeter, A., Edelman, A., and Kurlandzka, A. (2005) *Biochem. J.* **390,** 655–664
47. Kanter, U., Hauser, A., Michalke, B., Dräxl, S., and Schäffner, A. R. (2010) *J. Exp. Bot.* **61,** 3995–4009
48. Wegner, L. H., De Boer, A. H., and Raschke, K. (1994) *J. Membr. Biol.* **142,** 363–379
49. DeFelice, L. J., and Goswami, T. (2007) *Annu. Rev. Physiol.* **69,** 87–112
50. Fujisawa, M., Ito, M., and Krulwich, T. A. (2007) *Proc. Natl. Acad. Sci. U.S.A.* **104,** 13289–13294
51. Walker, D. J., Leigh, R. A., and Miller, A. J. (1996) *Proc. Natl. Acad. Sci. U.S.A.* **93,** 10510–10514
52. Serrano, R., Bernal, D., Simón, E., and Ariño, J. (2004) *J. Biol. Chem.* **279,** 19698–19704
53. Nelson, H., and Nelson, N. (1990) *Proc. Natl. Acad. Sci. U.S.A.* **87,** 3503–3507
54. Brodersen, D. E., Clemons, W. M., Jr., Carter, A. P., Morgan-Warren, R. J., Wimberly, B. T., and Ramakrishnan, V. (2000) *Cell* **103,** 1143–1154
55. Maresova, L., Urbankova, E., Gaskova, D., and Sychrova, H. (2006) *FEMS Yeast Res.* **6,** 1039–1046
56. Kinclova-Zimmermannova, O., Gaskova, D., and Sychrova, H. (2006) *FEMS Yeast Res.* **6,** 792–800
57. Sandoval, R. M., and Molitoris, B. A. (2004) *Am. J. Physiol. Renal Physiol.* **286,** F617–F624
58. Wagner, M. C., Molnar, E. E., Molitoris, B. A., and Goebl, M. G. (2006) *Antimicrob. Agents Chemother.* **50,** 587–595